Human Molecular Genetics, 2003, Vol. 12, No. 16 **1995–2001**
DOI: 10.1093/hmg/ddg213

Zinc metalloproteinase, *ZMPSTE24*, is mutated in mandibuloacral dysplasia

Anil K. Agarwal[1], Jean-Pierre Fryns[2], Richard J. Auchus[3] and Abhimanyu Garg[1]*

[1]Division of Nutrition and Metabolic Diseases, Department of Internal Medicine and Center for Human Nutrition, University of Texas Southwestern Medical Center, 5323 Harry Hines Blvd, Dallas, TX 75390, USA, [2]Center for Human Genetics, University Hospital of Leuven, Leuven, Belgium and [3]Division of Endocrinology, Metabolism and Diabetes, Department of Internal Medicine, University of Texas Southwestern Medical Center, Dallas, TX, USA

Received April 9, 2003; Revised June 9, 2003; Accepted June 17, 2003 DDBJ/EMBL/GenBank accession nos[†]

Mandibuloacral dysplasia (MAD; OMIM 248370) is a rare, genetically and phenotypically heterogeneous, autosomal recessive disorder characterized by skeletal abnormalities including hypoplasia of the mandible and clavicles, acro-osteolysis, cutaneous atrophy and lipodystrophy. A homozygous missense mutation, Arg527His, in the *LMNA* gene which encodes nuclear lamina proteins lamins A and C has been reported in patients with MAD and partial lipodystrophy. We studied four patients with MAD who had no mutations in the *LMNA* gene. We now show compound heterozygous mutations, Phe361fsX379 and Trp340Arg, in the zinc metalloproteinase (*ZMPSTE24*) gene in one of the four patients who had severe MAD associated with progeroid appearance and generalized lipodystrophy. ZMPSTE24 is involved in post-translational proteolytic cleavage of carboxy terminal residues of farnesylated prelamin A in two steps to form mature lamin A. Deficiency of Zmpste24 in mice causes accumulation of prelamin A and phenotypic features similar to MAD. The yeast homolog, Ste24, has a parallel role in processing of prenylated mating pheromone a-factor. Since human ZMPSTE24 can also process a-factor when expressed in yeast, we assessed the functional significance of the two *ZMPSTE24* mutations in the yeast to complement the mating defect of the haploid *MATa* yeast lacking *STE24* and Ras-converting enzyme 1 (*RCE1*; another prenylprotein-specific endoprotease) genes. The ZMPSTE24 mutant construct, Phe361fsX379, was inactive in complementing the yeast a-factor but the mutant, Trp340Arg, was partially active compared to the wild type ZMPSTE24 construct. We conclude that mutations in *ZMPSTE24* may cause MAD by affecting prelamin A processing.

INTRODUCTION

Mandibuloacral dysplasia (MAD) is a rare syndrome with variable clinical features including mandibular and clavicular hypoplasia, acro-osteolysis of terminal phalanges, delayed closure of cranial sutures, joint contractures, mottled pigmentation, cutaneous atrophy, lipodystrophy and features of metabolic syndrome such as insulin resistance, glucose intolerance, diabetes mellitus and hypertriglyceridemia (1). Previously, we described two patterns of lipodystrophy in patients with MAD: (i) type A pattern characterized by fat loss restricted to the extremities and (ii) type B pattern with more generalized fat loss (1). A homozygous missense mutation, Arg527His, in the *LMNA* gene was reported in Italian pedigrees with MAD and type A lipodystrophy (2). *LMNA* encodes lamins A and C by alternative splicing, which are integral components of nuclear lamina along with type B lamins (B1 and B2) which are encoded by two separate genes (3–5). Whereas type B lamins are expressed in all somatic cells, lamins A and C are preferentially expressed in differentiated cells (6). Precursors of lamins A, B1 and B2 have CAAX motif at the carboxy terminal and undergo post-translational modification including prenylation (5). However, lamin C lacks the carboxy-terminal CAAX motif and thus escapes prenylation. We sequenced *LMNA* in affected individuals from six pedigrees and found the Arg527His mutation in only two pedigrees with type A lipodystrophy (7). The remaining four pedigrees, in which the affected individuals showed type B lipodystrophy, revealed no mutations in the *LMNA* gene, suggesting additional genetic loci for MAD (7).

*To whom correspondence should be addressed at: University of Texas Southwestern Medical Center, 5323 Harry Hines Blvd, Dallas, TX 75390-9052, USA. Tel: +1 2146482895; Fax: +1 2146487150; Email: abhimanyu.garg@utsouthwestern.edu

[†]Human *ZMPSTE24*, AF064867.1; mouse *Zmpste24*, AAK 38172.1; Drosophila homolog, NP_611175.1; Arabidopsis *AtSTE24*, AF 353722; and *Saccharomyces cerevisiae STE24*, U77137.

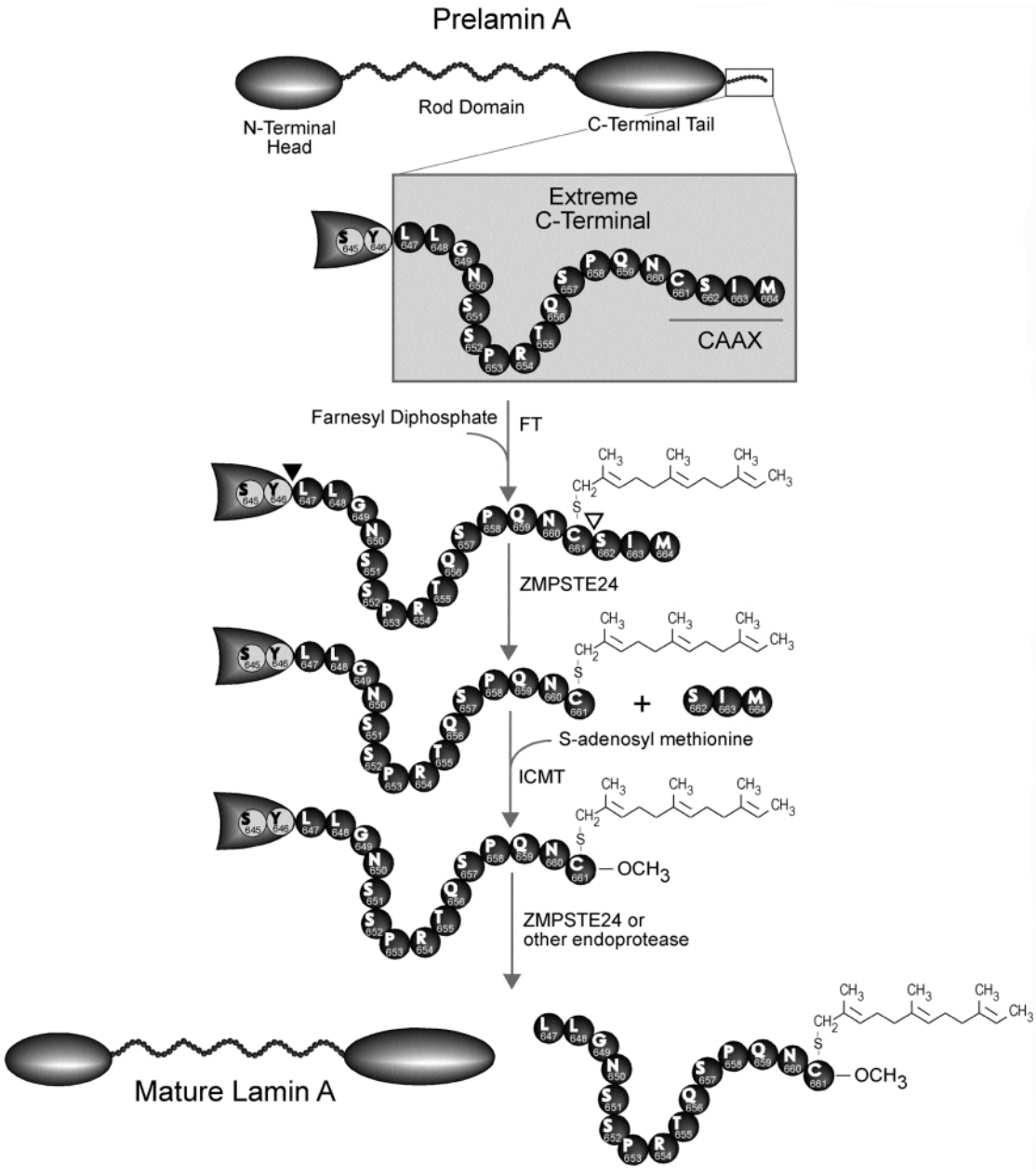

Figure 1. Schematic of steps involved in prelamin A processing to lamin A. The post-translational processing of prelamin A involves the extreme carboxy-terminal residues. In the first step, farnesyl diphosphate is used to farnesylate the cysteine in the conserved CAAX motif (CSIM in prelamin A) at the carboxy-terminal using the enzyme farnesyl transferase (FT). During the second step, the peptide bond between the cysteine and serine residues (indicated by an unfilled triangle) is proteolytically cleaved by ZMPSTE24, resulting in removal of SIM tripeptide. This reaction is followed by methylation of the farnesylated cysteine residue by isoprenylcysteine carboxyl methyl transferase (ICMT) using S-adenosyl methionine as the methyl donor. Finally, a second proteolytic cleavage occurs between the tyrosine and leucine residues (indicated by a filled triangle), which is either catalyzed by ZMPSTE24 or by another, as yet unidentified, endoprotease, and this cleavage removes 15 amino acids from the carboxy-terminal, resulting in formation of mature lamin A.

Recently, some of the phenotypic features of MAD (i.e. partial lipodystrophy and skeletal abnormalities including small mandible) were reported in mice with homozygous deletion of the gene encoding a zinc metalloproteinase, *Zmpste24* (8,9). Since Zmpste24 is involved in post-translational processing of prelamin A, the abnormal phenotypic features of *Zmpste24*$^{-/-}$ mice were attributed to defective processing of prelamin A (8,9). The generation of mature lamin A from prelamin A involves farnesylation of cysteine in the conserved CAAX motif at the carboxy-terminal (10) by the enzyme farnesyl transferase (Fig. 1). The AAX tripeptide is then proteolytically removed by ZMPSTE24, followed by methylation of the prenylated cysteine by isoprenylcysteine carboxyl methyl transferase. Finally, a second proteolytic cleavage, by ZMPSTE24 or

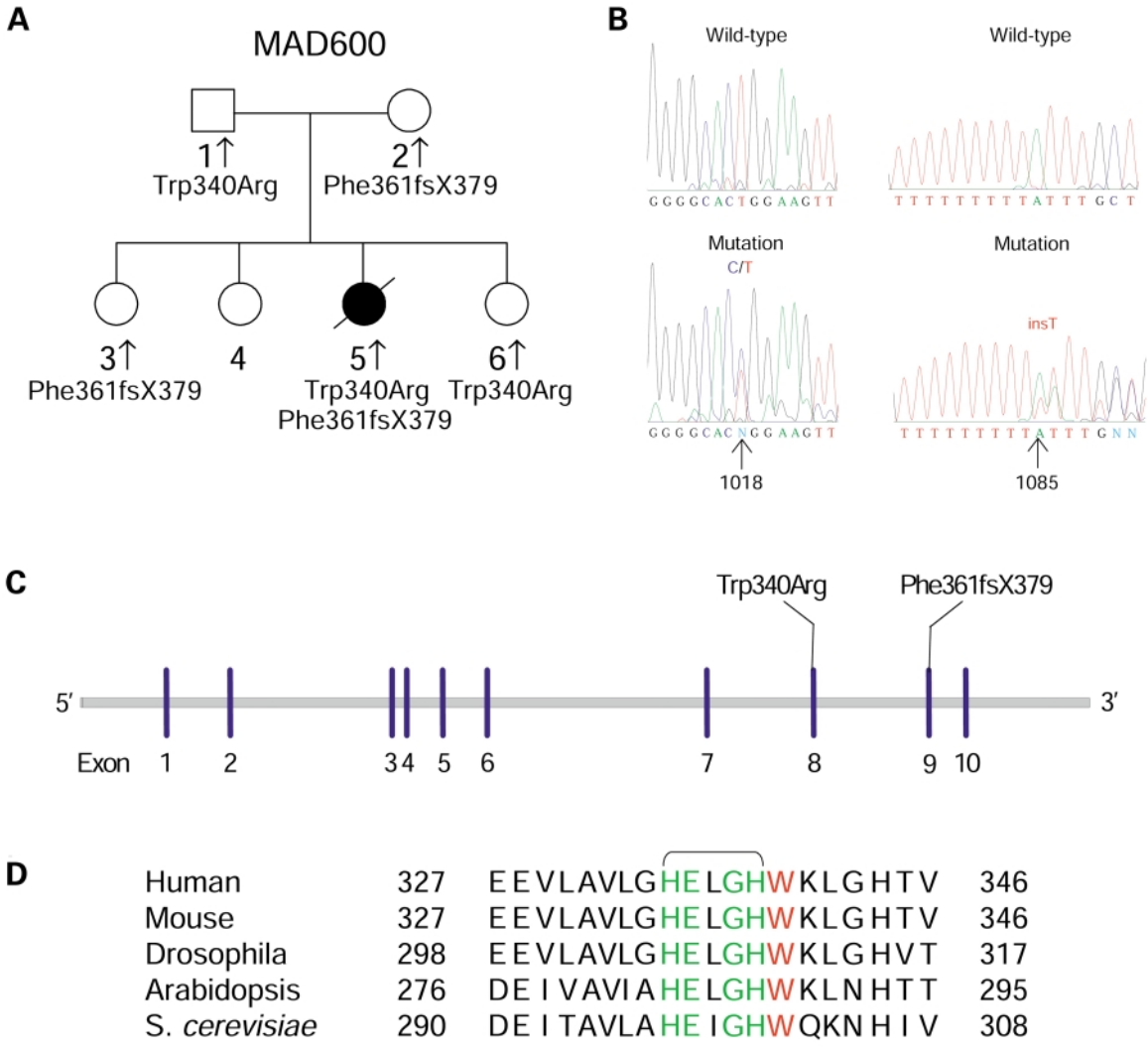

Figure 2. MAD 600 pedigree, sequence analysis, gene structure and conserved motifs of ZMPSTE24. (**A**) Pedigree of MAD 600 family with *ZMPSTE24* genotypes. No DNA was available from MAD 600.4. The mutations in *ZMPSTE24* are shown below the symbols. (**B**) Sequence electropherogram for mutations in exons 8 and 9 of *ZMPSTE24*. Identified mutations 1018T > C and 1085insT are marked by arrows and wild-type sequences are shown above for comparison. (**C**) The gene structure of *ZMPSTE24* and the location of the mutations in the patients with MAD. (**D**) Alignment of partial ZMPSTE24 sequences around the conserved motif HEXXH from human, mouse, Drosophila, Arabidopsis and *Saccharomyces cerevisiae*. This motif is located in exon 8 and is critical for proteolytic activity. The residue tryptophan at position 340, which is mutated in the patient with MAD, is located next to this motif (shown in green), and is conserved amongst species.

another protease, removes 15 amino acids from the carboxy-terminal (10) (Fig. 1). Given the role of ZMPSTE24 in prelamin A processing and the occurrence of a *LMNA* mutation in MAD subjects, we considered *ZMPSTE24* as a candidate gene and sequenced this locus in the remaining four patients.

RESULTS

We found compound heterozygous mutations in *ZMPSTE24* in a Belgian woman with severe MAD, progeroid appearance and lipodystrophy (Fig. 2A). One of the mutations, 1018T > C in exon 8, results in substitution of Trp at codon 340 to Arg (Fig. 2B). The second mutation, 1085insT in exon 9, causes a frameshift and a premature termination codon resulting in a truncated protein, Phe361fsX379. The parents and two siblings of the proband were healthy and were each heterozygous for one of the mutations (Fig. 2A). These mutations were not detected in 100 unrelated subjects of European ancestry. The other three MAD patients had no *ZMPSTE24* mutations. In these patients, we sequenced an additional gene encoding nuclear prelamin A recognition factor (NARF) which binds to prenylated prelamin A carboxy-terminal domain (11), but found no substantial alterations.

The human *ZMPSTE24* gene located on chromosome 1p34 spans ~43 kb with 10 exons that encode a 475 amino acid protein (Fig. 2C) (12,13). Exon 8 retains the conserved zinc metalloprotease motif, HEXXH, shown to be critical for proteolytic processing of proteins (12,14). The mutated residue, tryptophan 340, is adjacent to this motif and is conserved among species (Fig. 2D).

The human ZMPSTE24 protein was modeled for transmembrane spanning regions using the method developed by Jones

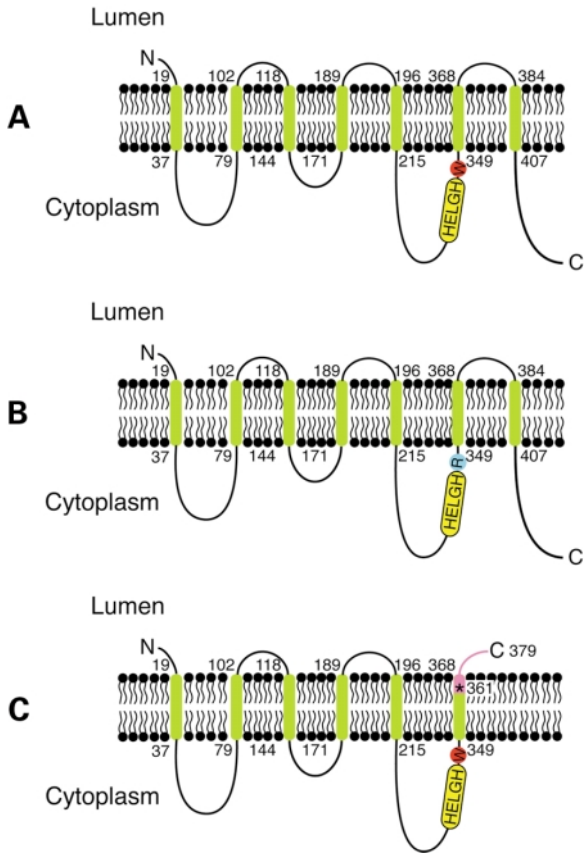

Figure 3. The predicted model of human ZMPSTE24 protein and the mutations. (**A**) The schematic of the protein shows seven transmembrane domains and the conserved zinc metalloprotease motif, HEXXH, which is critical for proteolytic processing of proteins. The catalytic motif and the carboxy terminus are on the cytoplasmic side. (**B**) The residue tryptophan 340, which is mutated to arginine, lies adjacent to the catalytic motif close to the membrane on the cytoplasmic side, but is not embedded in the membrane. (**C**) The first residue affected due to the frameshift mutation is phenylalanine 361, which lies within the sixth membrane spanning domain. This mutation leads to a truncated protein resulting in deletion of the seventh transmembrane domain as well as the carboxy terminal part of the protein. Thus the carboxyl terminal of the mutant protein is on the luminal side of the membrane and cannot participate in the catalytic action of the protease.

et al. (15) as shown in Figure 3A. The protein has seven transmembrane domains similar to the predicted domains of yeast ste24 (12). The residue tryptophan 340, which is mutated to arginine, lies adjacent to the catalytic motif close to the membrane on the cytoplasmic side, but is not embedded in the membrane (Fig. 3B). However, the frameshift mutation affects the phenylalanine 361 residue, which lies within the sixth membrane spanning domain and leads to a truncated protein (Fig. 3C). Thus, the carboxyl terminal of the mutant protein lies on the luminal side of the membrane and is not available for the catalytic action of the protease.

Ste24, a yeast homolog of ZMPSTE24, has a parallel role in the processing of prenylated mating pheromone **a**-factor (14,16). Ste24 not only functions as a carboxy-terminal CAAX protease, but is also necessary for proteolytic cleavage of seven amino-terminal residues from the **a**-factor precursor. Ras converting enzyme 1 (Rce1), a prenylprotein-specific

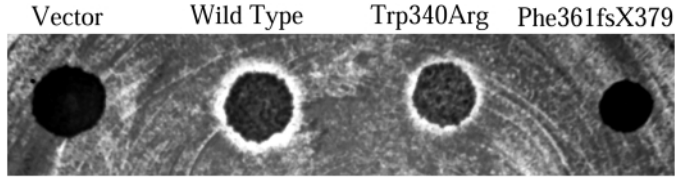

Figure 4. Yeast (*S. cerevisiae*) halo assay showing the mutant ZMPSTE24 partially or totally inactive in complementing the **a**-factor processing defect in *ste24Δrce1Δ* yeast (strain no. 3614). The *ste24Δrce1Δ* yeast strain was transformed with empty vector, pRS416GPD-*hZMPSTE24*-wild type and constructs, pRS416GPD-*hZMPSTE24*-Trp340Arg or pRS416GPD-*hZMPSTE24*-Phe361fsX379. Approximately 10^4 cells were spotted on to a lawn of yeast mating strain, XBH8-2C *MAT*α, grown on YPD, containing 0.04% Triton X-100. The *ste24Δrce1Δ* yeast with empty vector (vector) did not produce a zone of growth inhibition (halo) on the lawn of *MAT*α cells since they cannot produce mature **a**-factor. The expression vector containing human *ZMPSTE24* (wild-type) restored mature **a**-factor production and resulted in growth arrest of *MAT*α cells as judged by the halo surrounding the colony. The *ZMPSTE24* mutant, Trp340Arg resulted in a smaller halo compared to the wild type *ZMPSTE24*. The mutant Phe361fsX379 was unable to produce sufficient mature **a**-factor and produced no halo; however, at 10^6 cell concentration, a negligible halo was observed (data not shown).

CAAX protease, is also capable of carboxy-terminal processing of **a**-factor. Finally, another amino-terminal proteolytic cleavage mediated by Ax11 or Ste23 proteases yields a mature form of **a**-factor. Human *ZMPSTE24* expressed in yeast can also process **a**-factor and complement the mating defect of the haploid *MAT***a** yeast lacking the *STE24* and *RCE1* (*ste24Δrce1Δ*) genes (12,16). We therefore assessed the functional significance of the two *ZMPSTE24* mutations in the yeast complementation assay. In this assay, the secreted mature **a**-factor diffuses into the medium and arrests the growth of the *MAT*α strain leaving a 'halo' surrounding the *MAT***a** strain. The size of the halo is proportional to the production of the mature **a**-factor.

Figure 4 shows the results of the yeast halo assay assessing the complementation of the **a**-factor processing defect by transforming the *ste24Δrce1Δ* yeast with expression vectors for the wild type ZMPSTE24 or the mutations found in our subject. As expected, the *ste24Δrce1Δ* yeast with an empty vector did not produce a zone of growth inhibition (halo) on the lawn of *MAT*α cells since they cannot produce mature **a**-factor. The expression vector containing human *ZMPSTE24* (wild-type) restored mature **a**-factor production and resulted in growth arrest of *MAT*α cells as judged by the halo surrounding the yeast colony. The ZMPSTE24 mutant, Phe361fsX379, was inactive in complementing the yeast **a**-factor and produced no halo around the yeast colony consistent with the severe structural alteration of the protein (Fig. 3C). The mutant Trp340Arg, however, was partially active and produced a smaller halo compared to the wild type ZMPSTE24.

Our patient had a small chin, nose and mouth with poor postnatal growth in infancy (17). At age 2, skin atrophy and contractures on the limbs, delayed closure of anterior fontanelle, acro-osteolysis and clavicular hypoplasia were observed. She had a progeroid appearance with a pinched nose and multiple intracutaneous 'bony knots' on her fingers and toes that contained sclerotic tissue with calcification. At age 16, she had severe skin contractures around all of the interphalangeal joints, sparse and brittle hair, and mottled

pigmentation on the trunk. Skin on the face, head, arms and legs was very thin with underlying venous prominence suggesting generalized loss of subcutaneous fat (17). The progeroid appearance and skeletal changes were progressive and she also developed progressive glomerulopathy, which resulted in chronic renal failure necessitating dialysis. She died at age 24 due to pulmonary edema and malignant hypertension secondary to renal failure.

DISCUSSION

There are phenotypic similarities and differences between our patient with *ZMPSTE24* mutations and MAD subjects with *LMNA* mutation (2,7). Both types of patients have mandibular and clavicular hypoplasia, acro-osteolysis, joint contractures, skin atrophy and mottled pigmentation. Whereas MAD patients with *LMNA* mutation have normal development during the first 4–5 years, our patient developed skeletal abnormalities, skin atrophy and contractures at age 2. In contrast to MAD patients with *LMNA* mutation who have lipodystrophy of the extremities with sparing of the head and neck, our patient had generalized lipodystrophy affecting the face as well as extremities. The lack of subcutaneous fat from the face likely contributed to the progeroid appearance. In addition, our patient had 'bony knots' not observed in those with *LMNA* mutation.

Our patient also showed retarded growth and development and died prematurely, phenotypic features similar to those noted in the two lines of *Zmpste24*$^{-/-}$ mice (8,9). She also had scarce and brittle hair similar to the loss of fur in the *Zmpste24*$^{-/-}$ mice. However, instead of showing 'growth plate dysplasia' or bone fractures, our patient showed progressive mandibular and clavicular hypoplasia and acro-osteolysis of the distal phalanges. Although our patient had generalized lipodystrophy, there was no evidence of cardiomyopathy, abnormal gait or muscular dystrophy. Furthermore, our patient had severe progressive glomerulopathy which most likely was the reason for death. Although renal histopathology was not reported, in the end stage *Zmpste24*$^{-/-}$ mice serum creatinine levels were normal (8). 'Bony knots' on the phalanges and severe skin contractures were also peculiar features present in our patient. 'Bony knots' have only been rarely reported in patients with mandibuloacral dysplasia (18,19). Progeroid features have been previously described in patients with MAD and some of them were initially diagnosed as having Werner or progeroid syndrome (18,20–24). Recently, mutations in *LMNA* have been reported in patients with Hutchinson–Gilford progeria syndrome (HGPS), a rare genetic disorder characterized by features of premature ageing such as growth retardation, alopecia, atherosclerosis, sclerodermatous skin, and premature death during teenage years (25–27). Our data suggest that besides mutant forms of lamins A and C, defective processing of prelamin A due to *ZMPSTE24* mutations could also lead to progeroid features and early death.

Prelamin A is as yet the only recognized substrate of ZMPSTE24 in mammals; therefore, the clinical manifestations of the affected patient with *ZMPSTE24* mutations may be solely attributed to defective processing of prelamin A. However, abnormal or inadequate processing of other farnesylated proteins by ZMPSTE24, which might have additional roles including signal transduction, could be responsible for the unique phenotypic features of our patient. Although our patient had no documented evidence of dilated cardiomyopathy, muscular dystrophy and other skeletal disorders, which have been noted in *Zmpste24*$^{-/-}$ mice, *ZMPSTE24* mutations could result in phenotypic heterogeneity and may be implicated in these disorders (8,9). Finally, since three patients with MAD did not show any mutations in either the *LMNA* or the *ZMPSTE24* gene, other genetic loci may also be responsible for MAD, particularly those which interact with lamins A/C or are involved in the processing of lamin A.

MATERIALS AND METHODS

Patients and control subjects

We studied affected patients with MAD from four pedigrees. MAD 200 and 400 were of European origin from the US (1,28) and MAD 500 and 600 were from Belgium (17,29). All these patients had MAD with type B lipodystrophy pattern. One hundred normal healthy control subjects of European origin from the Dallas area were also studied by genotyping the mutations we found in *ZMPSTE24*. The protocol was approved by the appropriate Institutional Review Boards and all subjects gave informed consent.

Mutational analysis

Genomic DNA was isolated from the buffy coat by using DNAzol (Gibco, Gaithesburg, MD) according to the manufacturer's protocol. Specific primers were designed to amplify the exons and splice-site junctions of *ZMPSTE24* and *NARF*. The PCR reaction was assembled in a 50 µl reaction volume, containing 50 ng genomic DNA, 15 pmol of each primer, 1 × Premix D (Epicenter, Madison, WI) and 1 U of FailSafe Taq polymerase (Epicenter). PCR was carried out on PE9700 using the touchdown cycle protocol modified as follows: an initial denaturation at 98°C for 5 min, followed by a 3-step cycle (96°C for 30 s, 65°C* for 30 s, 72°C for 30 s) for 20 cycles (*0.5°C decrease with each cycle). This was followed for another 15 cycles as above except at an annealing temperature of 55°C. The PCR product was purified to remove primers and dNTPs and sequenced using ABI Prism 3100. Sequences were compared using Vector NTi Suite 6 software and by visual inspection. The 1085 insT mutation was further confirmed by subcloning in the PCR cloning vector pCR2.1 (Invitrogen, Carlsbad, CA) and sequencing four independent bacterial clones.

Genotyping

Exons 8 and 9 of *ZMPSTE24* were amplified from the 100 unrelated healthy subjects as described above and scored for the mutations seen in the patient with MAD. For the 1018T>C mutation in exon 8, which introduces a *Hpa*II restriction site, 5 µl of the PCR product was digested with *Hpa*II and the digest was resolved on the 3% agarose gel and visualized with EtBr, and a few samples were confirmed by direct sequencing. For the 1085insT, the PCR product was sequenced due to the lack of a convenient restriction site.

Table 1. Nucleotide sequences of the primers of *hZMPSTE24*

	Primer	Sequence
1	*hZMPSTE24*_101S	TCTGAAGGGACGAGTGTCGGTGTGG
2	*hZMPSTE24*_860AS	CCCTCAGGCAGAGGTGTGAATTTGT
3	*hZMPSTE24*_845S	CACCTCTGCCTGAGGGAAAGCTTAA
4	*hZMPSTE24*_1653AS	GGAACATGCTGCCAGGACAGAAATA
5	*hZMPSTE24*_XbaI	TGCTCTAGAATGGGGATGTGGGCATCGCTG
6	*hZMPSTE24*_XhoI	CCCTCGAGTCAGTGTTGCTTCATAGTTTT
7	*hZMPSTE24*_C_mut_S	GAACTGGGGCACCGGAAGTTGGGA
8	*hZMPSTE24*_C_mut_AS	TCCCAACTTCCGGTGCCCCAGTTC
9	*hZMPSTE24*_T_ins_S	GTGTTTTTTTTTTATTTGCTGTATTA
10	*hZMPSTE24*_T_ins_AS	TAATACAGCAAATAAAAAAAAAACAC

Cloning of human *ZMPSTE24* cDNA

The primers were designed for human *ZMPSTE24*, as shown in Table 1. The *ZMPSTE24* cDNA was amplified in two segments, using primer pairs 1 and 2 and primer pair 3 and 4, from the human liver Marathon Ready cDNA (BD Biosciences, Palo Alto, CA). The PCR was carried out as follows: an initial hold cycle for 2 min at 95°C, was followed for 20 cycles at 96°C for 30 s, 65°C* for 30 s, 72°C for 30 s for 20 cycles (*with a 0.5°C decrease in each cycle during annealing). This was followed by an additional 15 cycles at 94°C for 30 s, 55°C for 30 s and 72°C for 30 s. The PCR products of the above reactions were then mixed, and the second PCR was carried as above except using the outer primers 5 and 6 containing *Xba*I and *Xho*I restriction sites for cloning in a yeast expression vector. The PCR conditions were the same except that the extension time was increased to 1.5 min per cycle. The human *ZMPSTE24* cDNA and the yeast vector, pRS416GPD (30), were digested with *Xho*I and *Xba*I, gel purified and ligated. The resulting plasmid, pRS416GPD-h*ZMPSTE24*-wt, was sequenced to exclude PCR errors.

Mutant constructs

The *ZMPSTE24* mutations were generated using QuickChange mutagenesis kit (Stratagene, La Jolla, CA) as suggested by the manufacturer. The primers used with template pRS416GPD-hZMPSTE24-wt for the 1018T>C (primers 7 and 8) and 1085insT (primers 9 and 10) are shown Table 1. The resulting yeast expression vectors: pRS416GPD-h*ZMPSTE24*-Trp340Arg and pRS416GPD-h*ZMPSTE24*-Phe361fsX379, were again sequenced to ensure no additional PCR errors.

Growth arrest pheromone diffusion (halo) assay

To determine if the *ZMPSTE24* mutations are active in complementing the yeast *STE24*, the yeast expression plasmids pRS416GPD-h*ZMPSTE24*-Trp340Arg and pRS416GPD-h*ZMPSTE24*-Phe361fsX379 were transformed into yeast strain 3614 (*MATa ste24Δrce1Δ*) and grown on selective medium. Liquid cultures were concentrated, and 1 µl aliquots were then spotted onto a lawn of mating yeast (strain XBH8-2C, *MAT*α) on YPD medium with 0.04% Triton X-100 (31), and allowed to grow for 2 days at 30°C. The production of mature **a**-factor is proportional to the zone of growth inhibition (halo) formed.

ACKNOWLEDGEMENTS

We thank the members of the family for their invaluable contribution to this project; Drs S. Michaelis for yeast strain SM3614; B. Horazdovsky for yeast expression vector pRS416GPD and mating strain XBH8-2; E.A. Oral for DNA sample of MAD 200.3 and J. Cohen for providing DNA samples of control subjects; R. Barnes for the genome database search; T. Petricek, A. Osborn, R.G. Huet and R. Hall for management of DNA and patient databases, illustrations and technical assistance. The study was supported in part by the National Institutes of Health grants, R01-DK54387 and M01-RR00633, and by the Southwestern Medical Foundation.

REFERENCES

1. Simha, V. and Garg, A. (2002) Body fat distribution and metabolic derangements in patients with familial partial lipodystrophy associated with mandibuloacral dysplasia. *J. Clin. Endocrinol. Metab.*, **87**, 776–785.
2. Novelli, G., Muchir, A., Sangiuolo, F., Helbling-Leclerc. A., D'Apice, M.R., Massart, C., Capon, F., Sbraccia, P., Federici, M., Lauro, R. *et al.* (2002) Mandibuloacral dysplasia is caused by a mutation in *LMNA*-encoding lamin A/C. *Am. J. Hum. Genet.*, **71**, 426–431.
3. Lin, F. and Worman, H.J. (1993) Structural organization of the human gene encoding nuclear lamin A and nuclear lamin C. *J. Biol. Chem.*, **268**, 16321–16326.
4. Fisher, D.Z., Chaudhary, N. and Blobel, G. (1986) cDNA sequencing of nuclear lamins A and C reveals primary and secondary structural homology to intermediate filament proteins. *Proc. Natl Acad. Sci. USA*, **83**, 6450–6454.
5. Burke, B. and Stewart, C.L. (2002) Life at the edge: the nuclear envelope and human disease. *Nat. Rev. Mol. Cell Biol.*, **3**, 575–585.
6. Nigg, E.A., Kitten, G.T. and Vorburger, K. (1992) Targeting lamin proteins to the nuclear envelope: the role of CaaX box modifications. *Biochem. Soc. Trans.*, **20**, 500–504.
7. Simha, V., Agarwal, A.K., Oral, E.A., Fryns, J.-P. and Garg, A. (2003) Genetic and phenotypic heterogeneity in patients with mandibuloacral dysplasia-associated lipodystrophy. *J. Clin. Endocrinol. Metab.*, **88**, 2821–2824.
8. Pendas, A.M., Zhou, Z., Cadinanos, J., Freije, J.M., Wang, J., Hultenby, K., Astudillo, A., Wernerson, A., Rodriguez, F., Tryggvason, K. *et al.* (2002) Defective prelamin A processing and muscular and adipocyte alterations in Zmpste24 metalloproteinase-deficient mice. *Nat. Genet.*, **31**, 94–99.
9. Bergo, M.O., Gavino, B., Ross, J., Schmidt, W.K., Hong, C., Kendall, L.V., Mohr, A., Meta, M., Genant, H., Jiang, Y. *et al.* (2002) Zmpste24 deficiency in mice causes spontaneous bone fractures, muscle weakness, and a prelamin A processing defect. *Proc. Natl Acad. Sci. USA*, **99**, 13049–13054.
10. Sinensky, M., Fantle, K., Trujillo, M., McLain, T., Kupfer, A. and Dalton, M. (1994) The processing pathway of prelamin A. *J. Cell Sci.*, **107** (Pt 1), 61–67.

11. Barton, R.M. and Worman, H.J. (1999) Prenylated prelamin A interacts with Narf, a novel nuclear protein. *J. Biol. Chem.*, **274**, 30008–30018.
12. Tam, A., Nouvet, F.J., Fujimura-Kamada, K., Slunt, H., Sisodia, S.S. and Michaelis, S. (1998) Dual roles for Ste24p in yeast **a**-factor maturation: NH2-terminal proteolysis and COOH-terminal CAAX processing. *J. Cell Biol.*, **142**, 635–649.
13. Freije, J.M., Blay, P., Pendas, A.M., Cadinanos, J., Crespo, P. and Lopez-Otin, C. (1999) Identification and chromosomal location of two human genes encoding enzymes potentially involved in proteolytic maturation of farnesylated proteins. *Genomics*, **58**, 270–280.
14. Boyartchuk, V.L., Ashby, M.N. and Rine, J. (1997) Modulation of Ras and **a**-factor function by carboxyl-terminal proteolysis. *Science*, **275**, 1796–1800.
15. Jones, D.T., Taylor, W.R. and Thornton, J.M. (1994) A model recognition approach to the prediction of all-helical membrane protein structure and topology. *Biochemistry*, **33**, 3038–3049.
16. Schmidt, W.K., Tam, A. and Michaelis, S. (2000) Reconstitution of the Ste24p-dependent N-terminal proteolytic step in yeast **a**-factor biogenesis. *J. Biol. Chem.*, **275**, 6227–6233.
17. Schrander-Stumpel, C., Spaepen, A., Fryns, J.P. and Dumon, J. (1992) A severe case of mandibuloacral dysplasia in a girl. *Am. J. Med. Genet.*, **43**, 877–881.
18. Prasad, P.V., Padmavathy, L. and Sethurajan, S. (1998) Familial mandibuloacral dysplasia—a report of four cases. *Int. J. Dermatol.*, **37**, 614–616.
19. Danks, D.M., Mayne, V., Wettenhall, N.B. and Hall, R.K. (1974) Craniomandibular dermatodysostosis. *Birth Defects Orig. Artic. Ser.*, **10**, 99–105.
20. Welsh, O. (1975) Study of a family with a new progeroid syndrome. In Bergsma, D. (ed.), *New Chromosomal and Malformation Syndromes*, vol. 5. Liss, New York, pp. 25–38.
21. Parkash, H., Sidhu, S.S., Raghavan, R. and Deshmukh, R.N. (1990) Hutchinson-Gilford progeria: familial occurrence. *Am. J. Med. Genet.*, **36**, 431–433.
22. Cohen, L.K., Thurmon, T.F. and Slavaggio, J. (1973) Werner's syndrome. *Cutis*, **12**, 76–80.
23. Ramer, J.C. and Ladda, R.L. (1990) Report of a male with features overlapping geroderma osteodysplastica and mandibuloacral dysplasia. *Dysmorphol. Clin. Genet.*, **4**, 66–78.
24. Le Merrer, M., Guillot, M., Briard, M.L. and Maroteaux, P. (1991) Lethal progeroid syndrome with osteolysis. Case report. *Ann. Genet.*, **34**, 82–84.
25. Eriksson, M., Brown, W.T., Gordon, L.B., Glynn, M.W., Singer, J., Scott, L., Erdos, M.R., Robbins, C.M., Moses, T.Y., Berglund, P. *et al.*, (2003) Recurrent de novo point mutations in lamin A cause Hutchinson-Gilford progeria syndrome. *Nature*, **423**, 293–298.
26. Cao, H. and Hegele, R.A. (2003) LMNA is mutated in Hutchinson-Gilford progeria (MIM 176670) but not in Wiedemann–Rautenstrauch progeroid syndrome (MIM 264090). *J. Hum. Genet.*, **48**, 271–274.
27. De Sandre-Giovannoli, A., Bernard, R., Cau, P., Navarro, C., Amiel, J., Boccaccio, I., Lyonnet, S., Stewart, C.L., Munnich, A., Le Merrer, M. *et al.*, (2003) Lamin A truncation in Hutchinson–Gilford progeria. *Science*, e1084125.
28. Ng, D. and Stratakis, C.A. (2000) Premature adrenal cortical dysfunction in mandibuloacral dysplasia: a progeroid-like syndrome. *Am. J. Med. Genet.*, **95**, 293–295.
29. Vantrappen, G., Feenstra, L., Macours-Verelst, C. and Fryns, J.P. (2000) Mandibulo-acral dysplasia in a one-year-old boy. *Genet. Couns.*, **11**, 49–52.
30. Mumberg, D., Muller, R. and Funk, M. (1995) Yeast vectors for the controlled expression of heterologous proteins in different genetic backgrounds. *Gene*, **156**, 119–122.
31. Trueblood, C.E., Boyartchuk, V.L., Picologlou, E.A., Rozema, D., Poulter, C.D. and Rine, J. (2000) The CaaX proteases, Afc1p and Rce1p, have overlapping but distinct substrate specificities. *Mol. Cell. Biol.*, **20**, 4381–4392.